Phenomenology of neutral heavy leptons

Pat Kalyniak and I. Melo
Ottawa-Carleton Institute for Physics, Department of Physics, Carleton University, 1125 Colonel By Drive, Ottawa, Ontario, Canada K1S 5B6
(Received 8 July 1996)

We continue our previous work on the flavor-conserving leptonic decays of the Z boson with neutral heavy leptons (NHL's) in the loops by considering box, vertex, and self-energy diagrams for the muon decay. By inclusion of these loops (they contribute to the input parameter M_W), we can probe the full parameter space spanned by the so-called flavor-conserving mixing parameters $ee_{\rm mix}, \mu\mu_{\rm mix}, \tau\tau_{\rm mix}$. We show that only two diagrams from each class (box, vertex, and self-energy) are important; further, after renormalization only two box diagrams ''survive'' as dominant. We compare the results of our analysis with the existing work in this field and conclude that flavor-conserving decays have certain advantages over traditionally considered flavor-violating ones. [S0556-2821(97)02103-6]

PACS number(s): 14.60.St, 12.15.Ff, 13.35.Bv

I. INTRODUCTION

We have previously considered [1] a simple extension of the standard model (SM) with an enriched neutral fermion spectrum consisting of a massless neutrino and a Dirac neutral heavy lepton (NHL) associated with each generation [2–4]. Several parameters can be used to characterize the model: ''flavor-conserving'' mixing parameters $ee_{\rm mix}$, $\mu\mu_{\rm mix}$, $\tau\tau_{\rm mix}$; ''flavor-violating'' mixing parameters $e\mu_{\rm mix}$, $e\tau_{\rm mix}$, $\mu\tau_{\rm mix}$; and the mass scale M_N of NHL's (assuming three degenerate NHL's). We considered the effect, via these parameters, of NHL's on flavor-conserving Z boson decays to charged leptons and on the W boson mass M_W. However, in our earlier work, we neglected all mixing parameters except $\tau\tau_{\rm mix}$, which is the least well constrained. Here, we generalize our analysis by considering the case of arbitrary mixings $ee_{\rm mix}$, $\mu\mu_{\rm mix}$, and $\tau\tau_{\rm mix}$. Our previous neglect of $ee_{\rm mix}$ and $\mu\mu_{\rm mix}$ allowed us to also neglect a number of contributions to the muon decay corrections which feed into M_W as an input parameter. Including these couplings, non-SM box, vertex, and self-energy diagrams contributing to the muon decay (see Figs. 1, 2, 5) may become important for the calculation of M_W. In our previous paper [1], as a result of the assumption $ee_{\rm mix}=\mu\mu_{\rm mix}=0$, only oblique corrections (corrections to the W propagator) had to be considered. Here we consider the full set of corrections. Still, we assume here vanishing flavor-violating mixing parameters: $e\mu_{\rm mix}, e\tau_{\rm mix}, \mu\tau_{\rm mix}=0$. These parameters, if nonzero, lead to further complications, which in general require, as argued in a recent work [5], the renormalization of the mixing matrix. This is an interesting topic by itself; nevertheless, it is not crucial for our considerations. We note that the smallness of $e\mu_{\rm mix}$ is confirmed by experiment [6–11].

The inclusion of the arbitrary flavor-conserving mixing parameters completes our studies of the NHL's impact on the processes considered here. We compare our constraints on the parameters of the model with those coming from the traditionally favored flavor-violating processes, such as $\mu\to e\gamma$, $\tau\to eee$, $Z\to e\mu$, etc. [3,7–14]. We find that the processes we consider have certain advantages over the latter ones.

This paper is organized as follows. In Sec. II below, we briefly review a superstring-inspired $SU(2)_L\times U(1)_Y$ model of neutrino mass and the constraints on the mixings and masses of the model. In Sec. III, we present the additional muon decay corrections, identifying which contributions are important. Ultimately, our earlier results can primarily be improved by the tree-level modification of the vertex by mixing factors. In the limit of large M_N, only two box diagrams finally contribute but these are numerically only marginally important. Given the muon decay corrections, we also present the one-loop modification of the constraint on $\tau\tau_{\rm mix}$. In Sec. IV, we consider more generally the work done in this field. We contrast the sensitivity to the presence of NHL's in flavor-violating processes with the results for flavor-conserving processes. We include a calculation of the flavor-violating leptonic decays of the Z boson in our model. We summarize in Sec. V.

II. A SUPERSTRING-INSPIRED $SU(2)_L\times U(1)_Y$ MODEL OF NEUTRINO MASS

Here, we briefly describe the model of neutrino mass which we consider. For more details, we refer the reader to the original papers [2–4] or our previous work [1]. The model extends the neutral fermion sector of the SM by two new weak isosinglet neutrino fields (n_R, S_L) per generation. With total lepton number conservation imposed, the mass matrix is given by

$$-\mathcal{L}_{\rm mass}=\frac{1}{2}\mathcal{M}=\frac{1}{2}(\overline{\nu_L}\ \ \overline{n_L^c}\ \ \overline{S_L})\begin{pmatrix}0 & D & 0\\ D^T & 0 & M^T\\ 0 & M & 0\end{pmatrix}\begin{pmatrix}\nu_R^c\\ n_R\\ S_R^c\end{pmatrix}+\text{H.c.} \tag{1}$$

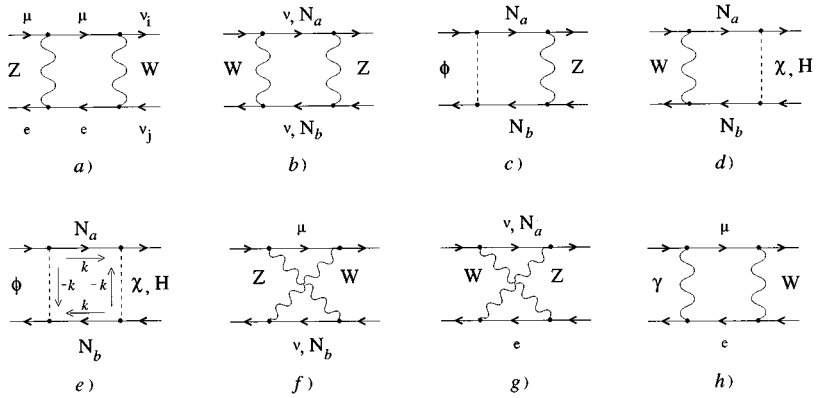

FIG. 1. Box diagrams for muon decay.

Each ν_L, n_R, S_L represents a collection of three fields, one for each family. D and M are 3×3 matrices. The diagonalization of the mass matrix yields three massless neutrinos (ν_i) along with three Dirac NHL's (N_a) of mass $M_N \sim M$. The weak interaction eigenstates ($\nu_l, l=e,\mu,\tau$) are related to the six mass eigenstates via a 3×6 mixing matrix $K\equiv(K_L, K_H)$:

$$\nu_l = \sum_{i=1,2,3} (K_L)_{li}\nu_{i_L} + \sum_{a=4,5,6} (K_H)_{la} N_{a_L}. \tag{2}$$

The mixing factor which typically governs flavor-conserving processes, $ll_{\rm mix}$, is given by

$$ll_{\rm mix} = \sum_{a=4,5,6} (K_H)_{la}(K_H^\dagger)_{al}, \quad l=e,\mu,\tau, \tag{3}$$

and the flavor-violating mixing factor $ll'_{\rm mix}$ is defined as

$$ll'_{\rm mix} = \sum_{a=4,5,6} (K_H)_{la}(K_H^\dagger)_{al'}, \quad l,l'=e,\mu,\tau, \quad l\neq l'. \tag{4}$$

Further, the following important inequality holds:

$$|ll'_{\rm mix}|^2 \leq ll_{\rm mix} l'l'_{\rm mix}, \quad l\neq l'. \tag{5}$$

This implies that one might observe nonstandard effects in flavor-conserving processes even if they are absent in flavor-violating processes.

We note here existing constraints on the parameter space of the model. *Indirect constraints* on the flavor-conserving mixing parameters $ee_{\rm mix}, \mu\mu_{\rm mix}, \tau\tau_{\rm mix}$ have been obtained from a global analysis of results including lepton universality measurements, Cabibbo-Kobayashi-Maskawa (CKM) matrix unitarity tests, W mass measurement, and measurements at the CERN e^+e^- collider LEP I. These constraints arise primarily at tree level due to the modification of couplings from those of the SM. Nardi *et al.* [15] have found the upper limits

$$ee_{\rm mix} \leq 0.0071, \quad \mu\mu_{\rm mix} \leq 0.0014, \quad \tau\tau_{\rm mix} \leq 0.033. \tag{6}$$

Since the limit on the parameter $\tau\tau_{\rm mix}$ plays (as the least stringent one so far) the most important role in our analysis, we will pay further attention to its source. The $\mu-\tau$ universality test is based on the τ leptonic decays compared to the μ leptonic decays, with the result given as the ratio of the couplings of τ and μ to the W boson, g_τ/g_μ. The tree-level ratio is found from

$$\frac{\Gamma(\tau\to e\nu\nu)/\Gamma^{\rm SM}(\tau\to e\nu\nu)}{\Gamma(\mu\to e\nu\nu)/\Gamma^{\rm SM}(\mu\to e\nu\nu)} = \left(\frac{g_\tau}{g_\mu}\right)^2 = \frac{1-\tau\tau_{\rm mix}}{1-\mu\mu_{\rm mix}}. \tag{7}$$

This measurement has undergone substantial improvement recently. With the most recent result $g_\tau/g_\mu = 0.9994 \pm 0.0028$ [16], the constraint on $\tau\tau_{\rm mix}$ is improved from its previous value of 0.033 by a factor of about 3. To reflect this improvement we present most of our results either for the values of $\tau\tau_{\rm mix}$ ranging from 0.033 to 0.01, or in a general form with $\tau\tau_{\rm mix}$ as a variable. In a few cases (e.g., when quoting results of others on flavor-violating processes), however, we only use $\tau\tau_{\rm mix}=0.033$. Finally, we note that these indirect limits depend very weakly on M_N; this point will be illustrated at the end of Sec. III.

Since NHL's have not been directly observed in the Z decay $Z\to N\nu$, we focus on NHL masses $M_N \gg M_Z, M_W, M_H$. These can be probed indirectly via *loop effects* in either flavor-violating or flavor-conserving processes. As argued in our previous work [1], only in this case are the contributions of NHL's via loops possibly significant, due to the violation of the Appelquist-Carazzone decoupling theorem [17]. Analogous to the behavior of the top quark loop contributions in the SM, quadratic nondecoupling (amplitudes $\sim M_N^2$) often results here.

III. NHL CONTRIBUTIONS TO MUON DECAY

A. Box diagrams

We first consider the box diagrams contributing to the muon decay, as depicted in Fig. 1. Diagrams of Figs. 1(b), 1(f), 1(g) each come in two varieties, with either massless neutrinos or NHL's in the loop. All diagrams without NHL's are similar to their SM counterparts; the only slight difference comes from the mixing factors in vertices (such as $1-ll_{\rm mix}$, see Appendix A). All the box graphs are finite.

The results of our computation of the diagrams of Figs. 1(a)–1(g) are given in Appendix A. [The QED box amplitude of Fig. 1(h), $\mathcal{M}_{\gamma eW\mu}$, is given in Ref. [18].] The dominant nonstandard contribution in the limit of $M_N \gg M_Z, M_W, M_H$ comes from just two graphs depicted in Fig. 1(e), one with Higgs boson H and one with neutral unphysical Higgs boson χ. To show that these two graphs

are dominant we could take the large M_N limit of the exact results given in Appendix A. We would find that only these two graphs exhibit quadratic nondecoupling, i.e., quadratic overall dependence on M_N. The remaining graphs with NHL's are either constant in the large M_N limit, or decouple as $1/M_N^2$. However, here we prefer a more intuitive approach based on dimensional analysis considerations and power counting.

The amplitude for the diagram with the Higgs boson H [Fig. 1(e)] is given by (we sum over NHL's N_a, N_b with $M_{N_a}=M_{N_b}=M_N$ and neglect external momenta in the internal propagators)

$$\mathcal{M}_{\phi NHN}=\sum_{a,b}\int\frac{dk^4}{(2\pi)^4}\overline{u}_{\nu_\mu}\frac{-ig_2}{2}\frac{M_N}{M_W}(K_L^\dagger K_H)_{ia}\times\frac{1+\gamma_5}{2}\frac{i}{\not k-M_N}\frac{ig_2}{2\sqrt{2}}\frac{M_N}{M_W}(K_H^\dagger)_{a\mu}\times(1-\gamma_5)u_\mu\overline{v}_e\frac{ig_2}{2\sqrt{2}}\frac{M_N}{M_W}(K_H)_{eb}\times(1+\gamma_5)\frac{i}{\not k-M_N}\frac{-ig_2}{2}\frac{M_N}{M_W}(K_H^\dagger K_L)_{bj}\times\frac{1-\gamma_5}{2}v_{\nu_e}\frac{i}{k^2-M_W^2}\frac{i}{k^2-M_H^2}. \tag{8}$$

Various mixing factors can be collected as

$$k_{\rm mix}\equiv(K_L^\dagger K_H)_{ia}(K_H^\dagger)_{a\mu}(K_H)_{eb}(K_H^\dagger K_L)_{bj}=(K_L^\dagger)_{i\mu}(K_L)_{ej}ee_{\rm mix}\mu\mu_{\rm mix}, \tag{9}$$

where we used $e\mu_{\rm mix}=\mu\tau_{\rm mix}=0$. Neglecting some constant factors which we will restore later, we get

$$\mathcal{M}_{\phi NHN}\sim M_N^4\int\frac{d^4k}{(2\pi)^4}\frac{k^2}{(k^2-M_N^2)^2(k^2-M_W^2)(k^2-M_H^2)}. \tag{10}$$

Note that the Lorentz structure of the amplitude is such that NHL propagators $i/(\not k-M_N)$ contribute as $i\not k/(k^2-M_N^2)$ rather than $iM_N/(k^2-M_N^2)$. In the limit of large M_N we can neglect all masses and momenta except M_N, obtaining

$$\mathcal{M}_{\phi NHN}\sim M_N^4\int\frac{d^4k}{(2\pi)^4}\frac{1}{(k^2-M_N^2)^2k^2}. \tag{11}$$

The integral is expected to be of the form $(M_N)^p$; power counting yields $p=-2$, so indeed the amplitude depends quadratically on M_N:

$$\mathcal{M}_{\phi NHN}\sim M_N^4M_N^{-2}=M_N^2. \tag{12}$$

We can further improve our estimate by restoring the constants collected from Eq. (8):

$$\mathcal{M}_{\phi NHN}=c\mathcal{M}_{\rm tree}\frac{\alpha}{s_W^2}\frac{M_N^2}{M_W^2}ee_{\rm mix}\mu\mu_{\rm mix}, \tag{13}$$

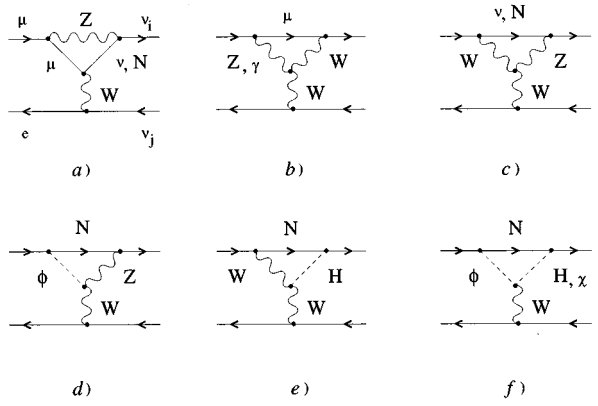

FIG. 2. Vertex diagrams for muon decay.

where

$$\mathcal{M}_{\rm tree}=-\frac{ig_2^2}{8M_W^2}[\overline{u}_{\nu_\mu}(1+\gamma_5)\gamma_\alpha u_\mu][\overline{v_e}(1+\gamma_5)\gamma^\alpha v_{\nu_e}]\times(K_L^\dagger)_{i\mu}(K_L)_{ej} \tag{14}$$

is the tree-level amplitude. The remaining numerical factor c can be found from the exact result given in Appendix A. It is equal to $c=1/64\pi$.

Similarly, the amplitude $\mathcal{M}_{\phi N\chi N}$ is, in the large M_N limit, equal to $\mathcal{M}_{\phi NHN}$. Dimensional analysis can also be applied to the remaining boxes, confirming that $\mathcal{M}_{\phi NHN}$ and $\mathcal{M}_{\phi N\chi N}$ are the only box diagrams with quadratic nondecoupling.

B. Vertex diagrams

We next consider together vertex corrections and corrections to the external charged leptons. Diagrams modifying the $W\mu\nu_i$ vertex are depicted in Fig. 2. Another set, one that modifies the $We\nu_j$ vertex, is not shown.

The sum over the depicted set of diagrams gives the muon vertex amplitude $\mathcal{M}^\mu_{\rm vertex}$:

$$\mathcal{M}^\mu_{\rm vertex}=\mathcal{M}_{\mu\nu Z}+\mathcal{M}_{\mu NZ}+\mathcal{M}_{ZW\mu}+\mathcal{M}_{\gamma W\mu}+\mathcal{M}_{WZ\nu}+\mathcal{M}_{WZN}+\mathcal{M}_{\phi ZN}+\mathcal{M}_{WHN}+\mathcal{M}_{\phi HN}+\mathcal{M}_{\phi\chi N}=\Lambda^\mu\mathcal{M}_{\rm tree}. \tag{15}$$

Explicit expressions for each of these amplitudes are given in Appendix A. They are divergent and we renormalize them with the SM form counterterms [18] (renormalized quantities are distinguished by the caret):

$$\hat{\Lambda}^\mu=\Lambda^\mu+\delta Z_1^W-\delta Z_2^W+\delta Z_L^\mu, \tag{16}$$

where

$$\delta Z_1^W-\delta Z_2^W=-\frac{\alpha}{2\pi s_W^2}\left(\frac{2}{\epsilon}-\gamma+\ln 4\pi-\ln\frac{M_W^2}{\mu^2}\right)=-\frac{\alpha}{2\pi s_W^2}\Delta_{M_W}, \tag{17}$$

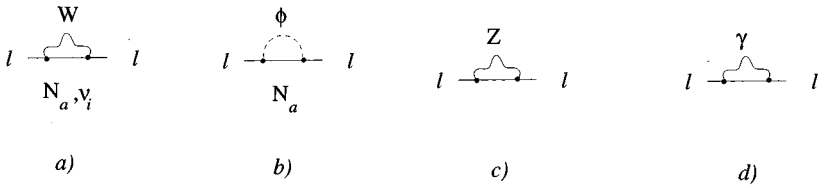

FIG. 3. Charged lepton self-energies.

$$\delta Z_L^{\mu} = -\Sigma_L^{\mu}(m_{\mu}^2) + \frac{\alpha}{2\pi}\left(2\ln\frac{m_{\mu}}{\lambda} - 1\right), \tag{18}$$

$2/\epsilon$ with $\epsilon \to 0$ is the pole of the dimensionally regularized amplitudes and λ is the regularized photon mass. $\Sigma_L^{\mu} = \Sigma_L^{WN} + \Sigma_L^{W\nu} + \Sigma_L^{\phi N} + \Sigma_L^{Z\mu} + \Sigma_L^{\gamma\mu}$ is the left-handed part of the muon self-energy, with the individual terms corresponding to the loops shown in Fig. 3. All these contributions are given in [1,18]. The term which we use specifically below, $\Sigma_L^{\phi N}$, is given in Appendix A. In our scheme, the renormalized charged lepton self-energies do not contribute directly, but rather through the renormalization constant δZ_L. Cancellation of divergences occurs as usual between the vertex loops and the counterterm contributions but we focus here on the M_N-dependent terms only. Looking for the dominant graphs in the limit $M_N \gg M_W, M_Z, M_H$, we find (either by taking the limit of exact results or using dimensional analysis and power counting) that the graphs of Fig. 2(f) have quadratic nondecoupling. However, both infinite and finite parts of these two graphs are canceled in the large M_N limit by the $\Sigma_L^{\phi N}$ term [see Fig. 3(b)] in the counterterm δZ_L^{μ} Therefore, there remain no M_N^2-dependent terms in the renormalized vertex diagrams.

This curious cancellation can be seen either explicitly (both $\Sigma_L^{\phi N}$ and $\mathcal{M}_{\phi HN}$, $\mathcal{M}_{\phi \chi N}$ are given in Appendix A) or, better yet, after applying the symmetries of the theory. The way to go is to study the more familiar case of a γll vertex. This vertex is modified from its tree-level value $ie\gamma_{\mu}$ by the one-loop diagrams shown in Fig. 4 as (we show only vector and axial-vector corrections)

$$ie\gamma_{\mu} \to ie\gamma_{\mu}(1 + F_V) - ie\gamma_{\mu}\gamma_5 F_A. \tag{19}$$

We now use a Ward identity [18,19], which relates the vertex form factors $F_{V,A}$ evaluated at $(p_1 + p_2)^2 = 0$ (p_1, p_2 are lepton momenta) to charged lepton self-energies represented by the counterterms $\delta Z_{V,A}^l$:

$$F_{V,A}(0) + \delta Z_{V,A}^l = \frac{1}{4 s_W c_W}\frac{\Sigma_{\gamma Z}(0)}{M_Z^2}, \tag{20}$$

where $\delta Z_V^l = \frac{1}{2}(\delta Z_L^l + \delta Z_R^l)$, $\delta Z_A^l = \frac{1}{2}(\delta Z_L^l - \delta Z_R^l)$, and $\Sigma_{\gamma Z}(0) = (\alpha/2\pi)(M_W^2/c_W s_W)\Delta_{M_W}$ is the term originating in the bosonic loops of the γ-Z mixing. At small M_N the graphs with unphysical Higgs boson ϕ are negligible; however, with $M_N \gg M_W, M_Z, M_H$ two types of graphs dominate the left-hand side of Eq. (20): the irreducible vertex (form factor) $F_{V,A}^{\phi\phi N}$ [see Fig. 4(c)] and the self-energy (its vector or axial-vector part) $\delta Z_{V,A}^{\phi N}$ (Fig. 3b). Since the right-hand side of Eq. (20) is not affected by the NHL's, it remains constant and (very) small with respect to $F_{V,A}^{\phi\phi N}$ or $\delta Z_{V,A}^{\phi N}$ at $M_N \sim 1$ TeV. Hence, the only way to meet the above formula is to have

$$F_{V,A}^{\phi\phi N} + \delta Z_{V,A}^{\phi N} = 0 \tag{21}$$

in the limit of large M_N. If we now return from the γll vertex to the $W\mu\nu$ vertex, we find a similar result (for proof see Appendix B):

$$\Lambda_{\phi HN} + \Lambda_{\phi \chi N} + \delta Z_L^{\phi N} = 0; \tag{22}$$

that is, the two dominant nonstandard contributions from Eq. (16) cancel exactly, including the finite parts. Since the remaining nonstandard contributions are not enhanced by the quadratic nondecoupling and are suppressed by the mixings, vertices can be reliably represented by the SM terms.

C. Neutrino self-energy and its renormalization

Half the neutrino self-energy diagrams contributing to muon decay are shown in Fig. 5. The corresponding self-energy is denoted as $\Sigma^{\nu_{\mu}}$. The other half consists of the same loops sitting on the bottom neutrino leg with the corresponding self-energy Σ^{ν_e}. In all these diagrams, we sum over the internal massless neutrinos $\nu_k, k = 1,2,3$. In principle, the graphs with ν_k replaced by N_a are also present; however, they are suppressed by the large mass M_N.

The unrenormalized neutrino self-energy Σ^{ν_l} $(l = e, \mu)$ has the form

$$\Sigma^{\nu_l} = \frac{1}{2}\Sigma_L^{\nu_l} \not{p}(1 - \gamma_5), \tag{23}$$

where $\Sigma_L^{\nu_l}$ receives contributions (given in Appendix A) from the diagrams of Fig. 5. The amplitude for those diagrams, in terms of $\Sigma_L^{\nu_l}$, can be shown to be equal to

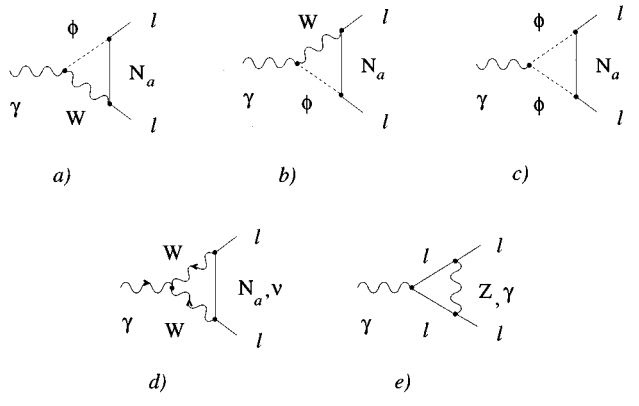

FIG. 4. γll vertex.

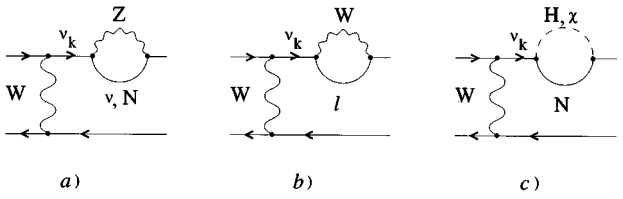

FIG. 5. Neutrino self-energy diagrams for muon decay.

$$\mathcal{M}_{\rm self} = -\mathcal{M}_{\rm tree}\frac{\Sigma_L^{\nu_l}}{2}, \tag{24}$$

where the factor $\frac{1}{2}$ comes from our dealing with the external wave function rather than the neutrino propagator.

Let us now investigate the question of the renormalization of Σ^{ν_l}. In this case the counterterms are modified from their SM form. The problem is how to renormalize a part of a theory where interaction eigenstates are different from mass eigenstates. Curiously, this also happens in the SM quark sector [20]. The difference is that in the SM the problem is circumvented by arguing that the off-diagonal quark mixings are too small to have any effect in the loops and the renormalization procedure is effectively simplified to that of mass eigenstates being also flavor eigenstates. In our model, we cannot neglect the ''off-diagonal'' mixings (their role is assumed by $ll_{\rm mix}$), since they (in combination with TeV NHL masses) lead to the dominant terms in the predicted deviation from SM results. This problem was studied in Refs. [5,20]. In Ref. [5] it was shown that, in general, the renormalization of the divergent amplitudes requires the renormalization of the mixing matrix. In our model, the amplitudes can be renormalized without the renormalization of the mixing matrix, if the assumption of zero flavor-violating mixing parameters is made. Our scheme is a straightforward extension of the SM counterterm.

We start with the counterterm Lagrangian, which has the same form as that of the SM,

$$i\,\delta Z_L^e\,\overline{\nu_e}\partial\!\!\!/\,\nu_e + i\,\delta Z_L^\mu\,\overline{\nu_\mu}\partial\!\!\!/\,\nu_\mu + i\,\delta Z_L^\tau\,\overline{\nu_\tau}\partial\!\!\!/\,\nu_\tau . \tag{25}$$

Weak eigenstates ν_l are given in terms of mass eigenstates ν_i, N_a in Eq. (2). This gives us, for the product $\overline{\nu_l}\nu_l$,

$$\overline{\nu_l}\nu_l = \sum_{k,i=1,2,3}\overline{\nu_i}(K_L^\dagger)_{il}(K_L)_{lk}\nu_k + \cdots(\overline{\nu_i}N, \overline{N}\nu_k, \overline{N}N), \tag{26}$$

and Eq. (25) thus contributes the massless neutrino counterterm

$$\sum_{k,i=1,2,3}\{\delta Z_L^e(K_L^\dagger)_{ie}(K_L)_{ek} + \delta Z_L^\mu(K_L^\dagger)_{i\mu}(K_L)_{\mu k} + \delta Z_L^\tau(K_L^\dagger)_{i\tau}(K_L)_{\tau k}\}\overline{\nu_i}\partial\!\!\!/\,\nu_k . \tag{27}$$

In our case we sum over internal ν_k but not over external ν_i. The graphic representation of the relevant counterterm (embedded in muon decay) is in Fig. 6.

The amplitude for this diagram is

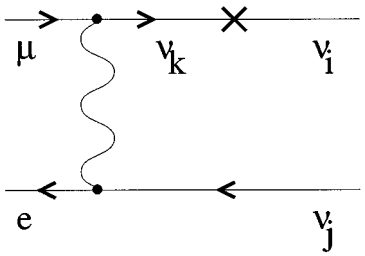

FIG. 6. Counterterm diagram for neutrino self-energy in muon decay.

$$\mathcal{M}_C = -\frac{1}{2}\mathcal{M}_{\rm tree}^{\rm SM}\sum_{l=e,\mu,\tau}\sum_{k=1,2,3} \times \delta Z_L^l (K_L^\dagger)_{il}(K_L)_{lk}(K_L^\dagger)_{k\mu}(K_L)_{ej} . \tag{28}$$

Again, the factor $\frac{1}{2}$ comes from our dealing with the external wave function rather than with the internal propagator. $\mathcal{M}_{\rm tree}^{\rm SM}$ is the tree-level amplitude for muon decay in the SM. The mixing factors $(K_L^\dagger)_{k\mu}$ and $(K_L)_{ej}$ originate at the $\mu W\nu_k$ and $eW\nu_j$ vertices, respectively. The amplitude $\mathcal{M}_C$ can be further simplified:

$$\begin{aligned}\mathcal{M}_C &= -\frac{1}{2}\mathcal{M}_{\rm tree}^{\rm SM}\sum_{l=e,\mu,\tau}\delta Z_L^l(K_L^\dagger)_{il}\sum_{k=1,2,3} \times (K_L)_{lk}(K_L^\dagger)_{k\mu}(K_L)_{ej} \\ &= -\frac{1}{2}\mathcal{M}_{\rm tree}^{\rm SM}\sum_{l=e,\mu,\tau}\delta Z_L^l(K_L^\dagger)_{il}(\delta_{l\mu} - l\mu_{\rm mix})(K_L)_{ej} \\ &= -\frac{1}{2}\mathcal{M}_{\rm tree}^{\rm SM}\delta Z_L^\mu(1-\mu\mu_{\rm mix})(K_L^\dagger)_{i\mu}(K_L)_{ej} \\ &= -\frac{1}{2}\,\delta Z_L^\mu(1-\mu\mu_{\rm mix})\mathcal{M}_{\rm tree} .\end{aligned} \tag{29}$$

The factor $(K_L^\dagger)_{i\mu}(K_L)_{ej}$ was absorbed by $\mathcal{M}_{\rm tree} = \mathcal{M}_{\rm tree}^{\rm SM}(K_L^\dagger)_{i\mu}(K_L)_{ej}$.

Now, we can write down the final expressions for the renormalized amplitude $\hat{\mathcal{M}}_{\rm self}$ and the renormalized neutrino self-energy $\hat{\Sigma}_L^{\nu_l}$:

$$\hat{\mathcal{M}}_{\rm self} = \mathcal{M}_{\rm self} + \mathcal{M}_C = -\frac{\Sigma_L^{\nu_l}}{2}\mathcal{M}_{\rm tree} - \frac{\delta Z_L^l}{2}(1-ll_{\rm mix})\mathcal{M}_{\rm tree} , \tag{30}$$

$$\hat{\Sigma}_L^{\nu_l} = \Sigma_L^{\nu_l} + \delta Z_L^l(1-ll_{\rm mix}). \tag{31}$$

The constant δZ_L^l was given in Eq. (18).

To prove the cancellation of the infinities, we note that the infinite part of δZ_L^l is given by [1,18]

$$\delta Z_L^{l,\infty} = -\frac{\alpha}{4\pi}\frac{1}{s_W^2}\left\{\frac{1}{2} + \frac{1}{4c_W^2} + \frac{M_N^2}{4M_W^2}ll_{\rm mix}\right\}\Delta_\mu , \tag{32}$$

where $\Delta_\mu = 2/\epsilon - \gamma + \ln 4\pi + \ln\mu^2$. The infinite part of the neutrino self-energy is (see Appendix A)

TABLE I. Contribution of the muon decay loops to δ_V, Δ_r, and M_W.

	SM	M_N = 0.5 TeV	M_N = 5 TeV	M_N = 15 TeV	M_N = 30 TeV	
		$ee_{\rm mix}=0.0071$,	$\mu\mu_{\rm mix}=0.0014$,	$\tau\tau_{\rm mix}=0.0$		
$\hat{\Sigma}^{\nu_e}+\hat{\Sigma}^{\nu_\mu}$	−4.995	−4.972	−4.982	− 4.988	−4.992	$\times10^{-2}$
$\hat{\Lambda}^{\mu}$	−1.441	−1.442	−1.444	− 1.444	−1.445	$\times10^{-2}$
$\mathcal{M}_{\rm box}/\mathcal{M}_{\rm tree}$	4.273	4.300	4.315	4.457	4.950	$\times10^{-3}$
δ_V	6.670	6.539	6.525	6.652	7.133	$\times10^{-3}$
$\hat{\Sigma}_W(0)/M_W^2$	2.396	2.346	2.301	1.872	0.329	$\times10^{-2}$
Δr	3.063	3.000	2.954	2.537	1.043	$\times10^{-2}$
M_W [GeV]	80.459	80.537	80.545	80.612	80.846	$\times1$
		$ee_{\rm mix}=0.0071$,	$\mu\mu_{\rm mix}=0.0014$,	$\tau\tau_{\rm mix}=0.033$		
δ_V	6.670	6.538	6.627	8.050	—	$\times10^{-3}$
$\hat{\Sigma}_W(0)/M_W^2$	2.396	2.363	1.209	−13.322	—	$\times10^{-2}$
Δr	3.063	3.017	1.871	−12.517	—	$\times10^{-2}$
M_W [GeV]	80.459	80.534	80.718	82.549	—	$\times1$

$$\Sigma_L^{\nu_l,\infty}=\frac{\alpha}{4\pi}\frac{1}{s_W^2}\left\{\frac{M_N^2}{4M_W^2}ll_{\rm mix}(1-ll_{\rm mix})+\frac{1}{2}(1-ll_{\rm mix})+\frac{1}{4c_W^2}ll_{\rm mix}(1-ll_{\rm mix})+\frac{1}{4c_W^2}(1-ll_{\rm mix})^2\right\}\Delta_\mu. \tag{33}$$

From the formulas above it can be easily seen that infinities cancel out in Eq. (31).

We now investigate the large M_N behavior of the renormalized neutrino self-energy $\hat{\Sigma}_L^{\nu_l}$, this time using exact results. The two diagrams of Fig. 5(c) contribute to the self-energy with an overall factor of M_N^2. For large M_N, the coefficients of these diagrams contain the functions

$$B_0(p;M_{H,Z,W},M_N)\sim 1-2\ln M_N,$$

$$B_1(p;M_{H,Z,W},M_N)\sim -0.25+\ln M_N. \tag{34}$$

This implies quadratic nondecoupling for $\Sigma_L^H(p)$ and $\Sigma_L^\chi(p)$ such that

$$\Sigma_L^H(p)+\Sigma_L^\chi(p)=\frac{\alpha}{2\pi}\frac{1}{4s_W^2}ll_{\rm mix}(1-ll_{\rm mix})\frac{M_N^2}{M_W^2}\times\left[\frac{1}{2}\Delta_\mu+\frac{3}{4}-\ln M_N\right]. \tag{35}$$

$\Sigma_L^{\phi N}$ [see Fig. 3(b)], which contributes to $\hat{\Sigma}_L^{\nu_l}$ via the counterterm δZ_L^l [see Eqs. (18) and (31)], is given in Appendix A [Eq. (A8)]. From here, we can see that (once again) $\Sigma_L^{\phi N}$ not only cancels infinities in $\Sigma_L^H(p)$ and $\Sigma_L^\chi(p)$, but, in the large M_N limit investigated, it also cancels the finite parts. As a result, there is no quadratic nondecoupling in the renormalized neutrino self-energy and, as in the case of irreducible vertex corrections, it suffices to consider just the SM loops.

D. Results

The loop corrections to muon decay modify the quantity Δr in the implicit relation between M_W and G_μ as [1]

$$M_W^2 s_W^2=\frac{\pi\alpha}{\sqrt{2}G_\mu(1-\Delta r)}\left(1-\frac{1}{2}ee_{\rm mix}-\frac{1}{2}\mu\mu_{\rm mix}\right), \tag{36}$$

where $1-\frac{1}{2}ee_{\rm mix}-\frac{1}{2}\mu\mu_{\rm mix}$ is the tree-level correction in our model and Δr can be written as

$$\Delta r=\frac{\mathcal{R}e\,\hat{\Sigma}_W(0)}{M_W^2}+\delta_V. \tag{37}$$

$\hat{\Sigma}_W(0)$ is the renormalized self-energy of the W boson which we previously calculated [1]. The parameter δ_V is the sum of the boxes, irreducible vertices, and self-energies calculated in the previous sections, along with the equivalent contributions to the $We\nu$ vertex,

$$\delta_V=\frac{\mathcal{M}_{\gamma eW\mu}+\mathcal{M}_{\rm box}}{\mathcal{M}_{\rm tree}}+\hat{\Lambda}^{\mu}+\hat{\Lambda}^{e}-\frac{1}{2}\hat{\Sigma}^{\nu_e}-\frac{1}{2}\hat{\Sigma}^{\nu_\mu}. \tag{38}$$

Based on the previous sections, we expect that δ_V can be reliably represented as

$$\delta_V\doteq\delta_V^{\rm SM}+\delta_b^{e\mu}=\delta_V^{\rm SM}+\frac{\alpha}{64\pi s_W^2}\frac{M_N^2}{M_W^2}ee_{\rm mix}\mu\mu_{\rm mix}, \tag{39}$$

where $\delta_V^{\rm SM}$ is the SM value [18] and the rest comes from just two box diagrams [Fig. 1(e)].

Numerical results for the corrections to muon decay are shown in Table I. As input data we used the following set (henceforth the standard set): $M_Z=91.1884$ GeV, $\alpha^{-1}=137.036$, $A\equiv\pi\alpha/\sqrt{2}G_\mu=37.281$ GeV, $M_H=200$ GeV, $m_t=176$ GeV. The mixing parameters used are $ee_{\rm mix}=0.0071$ and $\mu\mu_{\rm mix}=0.0014$ while for $\tau\tau_{\rm mix}$ we show results for both the minimal and the maximal value allowed, 0 and 0.033, respectively. $\tau\tau_{\rm mix}$ is the least well-constrained mixing; however, there is no particular theoretical motiva-

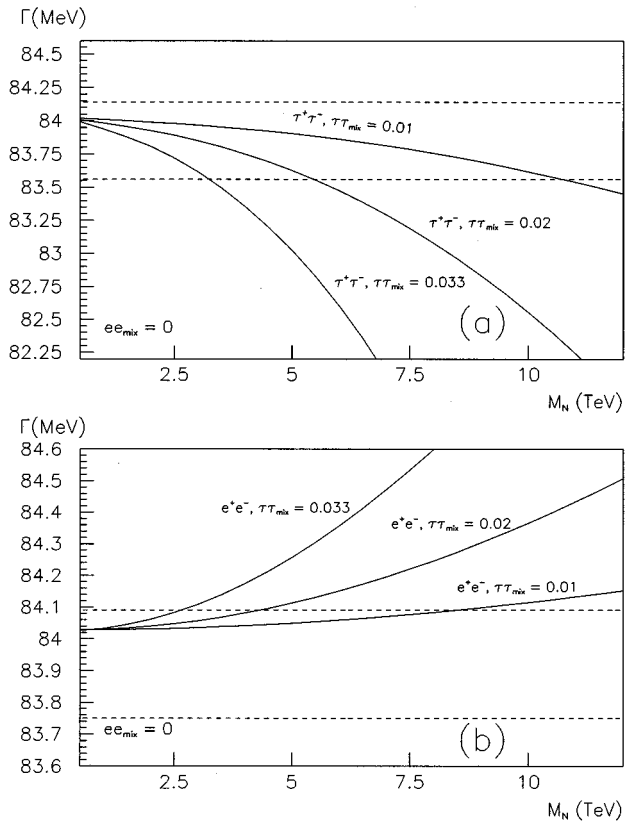

FIG. 7. Z leptonic width as a function of M_N for $ee_{\rm mix}=0$, $m_t=176$ GeV, Higgs boson mass $=200$ GeV, and different values of the mixing parameter $\tau\tau_{\rm mix}$: (a) $Z\to\tau\tau$ mode, (b) $Z\to ee$ mode. The dashed lines represent the 1σ band about the current experimental value (a) $\Gamma_{\tau\tau}^{\rm expt}=83.85\pm0.29$ MeV, (b) $\Gamma_{ee}^{\rm expt}=83.92\pm0.17$ MeV.

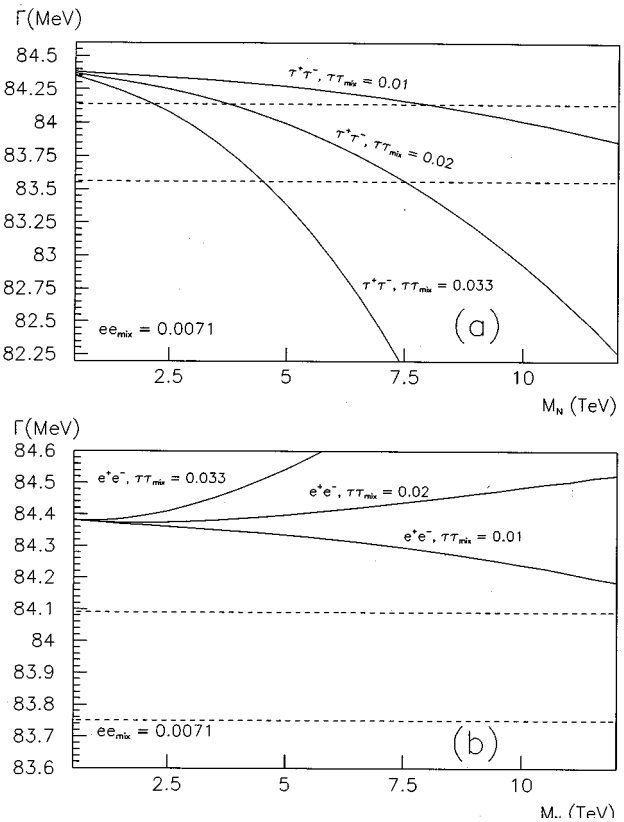

FIG. 8. Z leptonic width as a function of M_N for $ee_{\rm mix}=0.0071$, $m_t=176$ GeV, Higgs boson mass $=200$ GeV, and different values of the mixing parameter $\tau\tau_{\rm mix}$: (a) $Z\to\tau\tau$ mode, (b) $Z\to ee$ mode. The dashed lines represent the 1σ band about the current experimental value (a) $\Gamma_{\tau\tau}^{\rm expt}=83.85\pm0.29$ MeV, (b) $\Gamma_{ee}^{\rm expt}=83.92\pm0.17$ MeV.

tion to assume that it is actually larger than the other mixings. Hence, we give results with $\tau\tau_{\rm mix}$ suppressed in order to illustrate the dependence on $ee_{\rm mix}$ and $\mu\mu_{\rm mix}$. For $\tau\tau_{\rm mix}=0$ in the first three rows of the table we show the contributions of the self-energy, vertex, and box diagrams to δ_V (row 4) for NHL masses M_N of up to 30 TeV. Also shown (rows 5,6) are $\hat{\Sigma}_W(0)/M_W^2$ and Δr since, ultimately, we are interested in NHL effects in the observable M_W (row 7). The SM values are given in the first column. The results confirm expectations from the previous sections. There is no nondecoupling for self-energies and vertices and there is a quadratic dependence on M_N, in the large M_N limit, for the boxes. The boxes are becoming important at very high masses. Still, they are small compared to the change in $\hat{\Sigma}_W(0)/M_W^2$. This is due to the fact that the dominant boxes enter with the coefficient $ee_{\rm mix}\mu\mu_{\rm mix}$ [see Eq. (13)], while the correction to the W propagator is proportional to $k_{HH}=ee_{\rm mix}^2+\mu\mu_{\rm mix}^2+\tau\tau_{\rm mix}^2$ [1], which is allowed to be larger given the current bounds on the mixings. The W mass jumps from $M_W^{\rm SM}=80.459$ GeV to $M_W=80.537$ GeV at $M_N=0.5$ TeV, mainly as a result of the tree-level correction factor $(1-\frac{1}{2}ee_{\rm mix}-\frac{1}{2}\mu\mu_{\rm mix})$ [see Eq. (36)]. After that it rises very slowly until the M_N-dependent amplitudes become dominant above 5 TeV.

The results for $\tau\tau_{\rm mix}=0.033$ case (Table I, rows 8–11) are similar. We only show δ_V, $\hat{\Sigma}_W(0)/M_W^2$, Δr, and M_W since the boxes, self-energies, and vertices change slowly with $\tau\tau_{\rm mix}$ (they only depend implicitly on $\tau\tau_{\rm mix}$, via s_W), as illustrated by δ_V in row 8. The relative impact of non-SM boxes (δ_V) on Δr compared to that of $\hat{\Sigma}_W(0)/M_W^2$ decreases with increasing $\tau\tau_{\rm mix}$. $\hat{\Sigma}_W(0)/M_W^2\sim\tau\tau_{\rm mix}^2M_N^2$ corrections actually violate (for $M_N>5$ TeV) the perturbative unitarity bound discussed in Ref. [1] .

To sum it up, the analysis of Ref. [1] turns out to be basically valid even after the restriction $ee_{\rm mix}=\mu\mu_{\rm mix}=0$ is relaxed. The numerical predictions can be improved by the inclusion of the tree-level correction $(1-\frac{1}{2}ee_{\rm mix}-\frac{1}{2}\mu\mu_{\rm mix})$, while the largest loop corrections, the box diagrams of Fig. 1e, are only marginally important. Only in the case of the Z decay into e^+e^-, with $ee_{\rm mix}$ and $\tau\tau_{\rm mix}$ now made comparable, does the character of the M_N dependence change (see below).

The impact of these results is shown in Figs. 7 and 8. We give the Z leptonic widths as a function of NHL mass for the two cases, $ee_{\rm mix}=0$ and $ee_{\rm mix}=0.0071$, ($\mu\mu_{\rm mix}$ is negligible) in Figs. 7 and 8, respectively. These figures show the widths for three values of $\tau\tau_{\rm mix}$: 0.033, 0.02, and 0.01. The remaining input data come from the standard set. The dashed lines represent the 1σ variation about the current experimental results for the individual Z leptonic widths,

TABLE II. Flavor-violating decays: experimental limits, theoretical predictions, and the constraints implied.

Process	Experimental B [6]	Theoretical B	Limits on masses and/or mixings
$\mu\to e\gamma$	$\leqslant 4.9\times10^{-11}$ 90% C.L.	4.9×10^{-11} [a]	$\lvert e\mu_{\rm mix}\rvert\leqslant 0.00024$
$\tau\to e\gamma$	$\leqslant 1.2\times10^{-4}$ 90% C.L.	7×10^{-7} [b]	—
$\tau\to \mu\gamma$	$\leqslant 4.2\times10^{-6}$ 90% C.L.	7×10^{-7} [b]	—
$\mu\to eee$	$\leqslant 1.0\times10^{-12}$ 90% C.L.	1.0×10^{-12} [c]	$M_N^2\leqslant 0.93\times10^{-5}\,\dfrac{1\ \text{TeV}^2}{ee_{\rm mix}\lvert e\mu_{\rm mix}\rvert}$
$\tau\to eee$	$\leqslant 1.4\times10^{-5}$ 90% C.L.	5×10^{-7} [d]	—
$\tau\to e\mu\mu$	$\leqslant 1.4\times10^{-5}$ 90% C.L.	3×10^{-7} [d]	—
$Z\to e\mu$	$\leqslant 6.0\times10^{-6}$ 95% C.L.	3.3×10^{-8} [e]	—
$Z\to e\tau$	$\leqslant 1.3\times10^{-5}$ 95% C.L.	1.4×10^{-6} [e]	—
$Z\to \mu\tau$	$\leqslant 1.9\times10^{-5}$ 95% C.L.	2.2×10^{-7} [e]	—

[a] $\lvert e\mu_{\rm mix}\rvert=0.00024,\ \ M_N>0.5$ TeV; Ref. [9].
[b] $ee_{\rm mix}=0.043, \mu\mu_{\rm mix}=0.008, \tau\tau_{\rm mix}=0.1,\ \ M_N>0.5$ TeV; Ref. [9].
[c] $M_N^2\times ee_{\rm mix}\lvert e\mu_{\rm mix}\rvert=0.93\times10^{-5}\times1\ \text{TeV}^2$; Ref. [11].
[d] $ee_{\rm mix}=0.01, \mu\mu_{\rm mix}=0, \tau\tau_{\rm mix}=0.033, M_N=3$ TeV; Ref. [14].
[e] $ee_{\rm mix}=0.0071, \mu\mu_{\rm mix}=0.0014, \tau\tau_{\rm mix}=0.033, M_N=5$ TeV; this paper and Ref. [14].

$\Gamma_{\tau\tau}^{\rm expt}=83.85\pm0.29$ MeV and $\Gamma_{ee}^{\rm expt}=83.92\pm0.17$ MeV [21]. The one-loop SM prediction is $\Gamma_{\tau\tau}=\Gamma_{ee}=84.03$ MeV.

We have discussed the main features of Figs. 7(a) and 7(b) ($\Gamma_{ll}\sim\tau\tau_{\rm mix}^2M_N^2$, rising Γ_{ee} vs falling $\Gamma_{\tau\tau}$ for $\tau\tau_{\rm mix}$ dominating $ee_{\rm mix}$) previously [1]. Here, we point out that the main difference between Figs. 7(a) and 7(b) and Figs. 8(a) and 8(b), namely, the total upward shift of the widths in the latter, can indeed be traced to the tree-level correction to the μ decay. Unfortunately, this tree-level correction interferes destructively with the one-loop corrections which drive $\Gamma_{\tau\tau}$ widths down. Also note that as $\tau\tau_{\rm mix}$ and $ee_{\rm mix}$ become comparable, so do $\Gamma_{\tau\tau}$ and Γ_{ee}, as expected.

Our best constraints at the 2σ level on NHL mass come from $\Gamma_{\tau\tau}$, shown in Fig. 7(a);[1] we get $M_N\leqslant4.3$ TeV for $\tau\tau_{\rm mix}=0.033$, $M_N\leqslant7$ TeV for $\tau\tau_{\rm mix}=0.02$, and $M_N\leqslant13$ TeV for $\tau\tau_{\rm mix}=0.01$. These constraints can be neatly summarized in the approximation

$$M_N\leqslant4.3\times\frac{0.033}{\tau\tau_{\rm mix}}\ \ \text{TeV}. \tag{40}$$

Here, this assumes $\tau\tau_{\rm mix}$ dominates $ee_{\rm mix}$.

We note that as the value of $\tau\tau_{\rm mix}$ is more tightly constrained, these limits are less restricted than those from perturbative unitarity considerations [1]:

$$M_N\leqslant4\times\sqrt{0.033/\tau\tau_{\rm mix}}\ \ \text{TeV}. \tag{41}$$

Finally, we note that our computation of the muon decay loops also enables us to find the one-loop modification of Eq. (7) by NHL's:

$$\frac{\Gamma(\tau\to e\nu\nu)/\Gamma^{\rm SM}(\tau\to e\nu\nu)}{\Gamma(\mu\to e\nu\nu)/\Gamma^{\rm SM}(\mu\to e\nu\nu)}=\left(\frac{g_\tau}{g_\mu}\right)^2=\frac{1-\tau\tau_{\rm mix}}{1-\mu\mu_{\rm mix}}\,\frac{1+2\,\delta_b^{e\tau}}{1+2\,\delta_b^{e\mu}}, \tag{42}$$

where δ_b is given in Eq. (39). For $M_N=4$ TeV, and the current constraints on the mixing parameters, we find that the one-loop correction is only about 1% of the tree-level correction; therefore, the constraints of Ref. [15] are indeed independent of the NHL mass.

IV. FLAVOR-CONSERVING VS FLAVOR-VIOLATING DECAYS

In this section, we review the constraints on the parameters in our model as derived from flavor-violating and flavor-conserving decays (the latter will be represented by the leptonic decays of the Z boson). We compare the sensitivity of these two classes of processes to the presence of NHL's.

Lepton flavor-violating decays have so far received a lot more attention [3,7–14] than the flavor-conserving processes [1,22]. The calculation of the flavor-violating processes is simpler, with a smaller number of contributing diagrams and without the need to renormalize. Also, there could be a certain preconception that the experimental signature of the flavor violation is more ''dramatic.'' It is our intention to show here that in many cases this expectation is not justified. We give also the results of our calculation of flavor-violating decays of the Z boson. A summary of experimental limits, theoretical predictions, and the constraints on the mixings and/or NHL masses implied by flavor-violating decays is given in Table II. We will now address these decays one by one.

In the case of the flavor-violating mixing parameters, the constraint on one of them, $e\mu_{\rm mix}$, arises from the measured limit of a rare decay $\mu\to e\gamma$. This decay was studied in the context of our model and of seesaw models with enhanced mixings (an example of a seesaw model with enhanced mixings is the model of Ref. [23]) by several authors [7–11]. The $\mu\to e\gamma$ branching ratio goes like $\lvert e\mu_{\rm mix}\rvert^2$ times a function which is independent of M_N for $M_N>500$ GeV. The current experimental limit on the $\mu\to e\gamma$ branching ratio, $B_{\rm expt}\leqslant4.9\times10^{-11}$ [6], yields a very stringent upper limit on the mixing of $\lvert e\mu_{\rm mix}\rvert\leqslant0.00024$ (see Table II).

[1] Constraints from Γ_{ee} shown in Fig. 7(b) are just slightly worse at the 2σ level.

One might expect the other flavor-violating mixing parameters, $e\tau_{\rm mix}$ and $\mu\tau_{\rm mix}$, to be limited by the corresponding flavor-violating τ decays. However, experimental limits on $\tau\to e\gamma$ and $\tau\to\mu\gamma$, $B_{\rm expt}\leqslant 1.2\times10^{-4}$, $B_{\rm expt}\leqslant 4.2\times10^{-6}$, respectively [6], are much weaker. Moreover, the predicted rate $B_{\rm th}=7\times10^{-7}$ [9] is now out of date due to improved constraints on the mixings (see Table II). With the current limit ($\tau\tau_{\rm mix}=0.033$), the predicted rate would be smaller by at least one order of magnitude, implying that the theoretical result is two orders of magnitude below the experimental upper limit for $\mu\gamma$ mode and about three orders for $e\gamma$ mode. As a result, it is not these flavor-violating processes which place the strongest limits on the flavor-violating mixing parameters. Rather, for $\mu\tau_{\rm mix}$ and $e\tau_{\rm mix}$, we have to use indirect limits obtained by combining the global analysis results for the flavor-conserving mixing parameters with the inequality, Eq. (5).

Several other flavor-violating processes at very low energies have been considered. Another well-constrained muon decay mode is $\mu\to e^-e^-e^+$ ($B_{\rm expt}\leqslant 1.0\times10^{-12}$, [6]), studied in Refs. [7,8,10,11]. The calculation shows the quadratic nondecoupling which we will encounter in the lepton flavor-violating decays of the Z boson below. Reference [11] gives (with an assumption discussed therein) the following constraint on NHL mass as a function of $ee_{\rm mix}, e\mu_{\rm mix}$ (see Table II):

$$M_N^2\leqslant 0.93\times10^{-5}\,\frac{1\ \ {\rm TeV}^2}{ee_{\rm mix}|e\mu_{\rm mix}|}. \tag{43}$$

Also considered in Refs. [7,8,11] is $\mu-e$ conversion in nuclei, $\mu^-(A,Z)\to e^-(A,Z)$. The resulting constraint on the product $ee_{\rm mix}|e\mu_{\rm mix}|$ [11] is similar to the one above.

For the flavor-violating decays of the τ into three leptons ($\tau\to e^-e^-e^+$, $e^-\mu^-\mu^+$, etc.) we know of no calculation studying the large (TeV) NHL mass limit in the context of our model. However, within the seesaw model of Ref. [23], Pilaftsis [14] predicts with the current limits on mixings ($\tau\tau_{\rm mix}=0.033$) and for $M_N=3$ TeV rates $B_{\rm th}(\tau\to e^-e^-e^+)=5\times10^{-7}$, $B_{\rm th}(\tau\to e^-\mu^-\mu^+)=3\times10^{-7}$ which are well below the current experimental limit $B_{\rm expt}\leqslant 1.4\times10^{-5}$ [6] (see Table II).

Finally, hadronic decay modes of the τ lepton, $\tau\to l\eta, l\pi^0$ [9] are also disfavored by loose limits, e.g., $B_{\rm expt}(\tau\to\mu^-\pi^0)\leqslant 4.4\times10^{-5}$ [6].

Consider now the case of the flavor-violating leptonic decays of the Z boson. These rare processes were studied in the context of our model previously [3,12]; however, the limit of large NHL mass was not fully investigated. This point was noted in Ref. [13], where the branching ratios for $Z\to l_1^-l_2^+$ ($e^\pm\mu^\mp,\mu^\pm\tau^\mp,e^\pm\tau^\mp$) were derived in the seesaw model of Ref. [23]. We, therefore, here present the results in our model, having carefully treated the case of a large NHL mass but without showing the calculational details. The loop diagrams involved are very similar to those of the flavor-conserving leptonic decays of the Z boson which we discussed fully in Ref. [1] and the calculation of the flavor-violating process is very similar to that of Ref. [13] for the other model. The particular predictions depend, along with the NHL mass, on the various mixings and their relative phases. We do not present full details here since the results are not particularly promising. The branching ratio

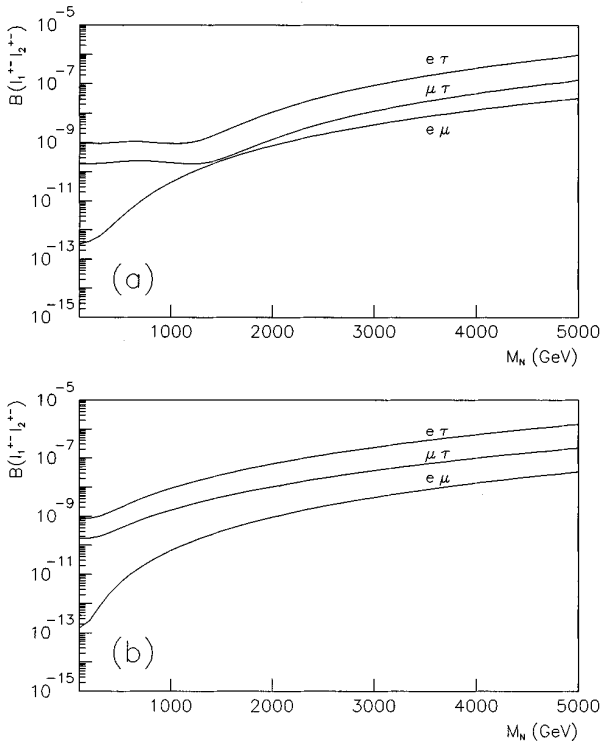

FIG. 9. The branching ratio $Z\to l_1^\pm l_2^\mp$ as a function of M_N for (a) $\delta=-1$, (b) $\delta=+1$.

$B(l_1^\pm l_2^\mp)\equiv\Gamma_{l_1^+l_2^-+l_1^-l_2^+}/\Gamma_Z$ is shown as a function of M_N in Figs. 9(a) and 9(b). The parameter δ introduced in these figures corresponds to the allowed range of relative phases arising in the mixing factors. In Fig. 9(a), we set $\delta=-1$ and in Fig. 9(b), $\delta=+1$.

As an example for comparison with experiment, using maximally allowed mixings ($\tau\tau_{\rm mix}=0.033$) and $\delta=+1$, we predict the following branching ratio limits for $M_N=5$ TeV:

$$\begin{aligned} &B_{\rm th}(Z\to e^\pm\mu^\mp)<3.3\times10^{-8},\\ &B_{\rm th}(Z\to e^\pm\tau^\mp)<1.4\times10^{-6},\\ &B_{\rm th}(Z\to \mu^\pm\tau^\mp)<2.2\times10^{-7}. \end{aligned} \tag{44}$$

These results are similar to those of Ref. [14], where, as noted above, the calculation was done in the context of a seesaw model with enhanced mixings. For experimental limits see Table II. Our most promising prediction, for the $e\tau$ mode, is at least one order of magnitude below the experimental limit. Hence, the flavor-violating leptonic decays of the Z boson do not represent a good chance for finding evidence of NHL's.

We conclude that the flavor-violating processes give only one (mixing-dependent) constraint on NHL mass[2] coming from $\mu\to eee$ (or $\mu-e$ conversion in nuclei), see Eq. (43). For $ee_{\rm mix}=0.0071$ and $|e\mu_{\rm mix}|=0.00024$, this yields $M_N<2.3$ TeV. For the remaining flavor-violating processes to become sensitive to NHL mass, the experimental upper limits would have to be pushed down by at least one order of

[2]The extremely useful limit on $e\mu_{\rm mix}$ arising from $\mu\to e\gamma$, is not sensitive to M_N, for $M_N>500$ GeV.

magnitude for flavor-violating leptonic decays of the Z boson, and by one to two orders of magnitude for flavor-violating decays of the τ lepton. This most likely requires increased high luminosity running at LEP I energy and a τ factory [24].

On the other hand, the flavor-conserving processes lead to limits on M_N summarized in Eq. (40), which for $\tau\tau_{\rm mix}=0.033$ give $M_N<4.3$ TeV. These limits depend on different mixing parameters than the flavor-violating constraint and thus probe a different part of the mixings vs NHL mass parameter space. A disadvantage of the flavor-violating decays is that they are always proportional to a flavor-violating parameter and this can lead, via the inequality [Eq. (5)], to their further suppression with respect to flavor-conserving processes. It is perfectly possible that there might be signatures of the flavor-conserving processes even if there is no sign of the flavor-violating ones.

V. CONCLUSIONS

In this paper, we have generalized our previous analysis of a model containing NHL's by relaxing the restriction on mixing parameters $ee_{\rm mix}=\mu\mu_{\rm mix}=0$. This involved evaluating one-loop corrections to the muon decay which feed into the input parameter M_W. We found that two box diagrams exhibit quadratic nondecoupling but that they are only marginally important numerically. Hence, the numerical results of Ref. [1] remain basically valid, although they can be improved by the inclusion of the tree-level correction to the muon decay, $(1-\frac{1}{2}ee_{\rm mix}-\frac{1}{2}\mu\mu_{\rm mix})$.

The mass M_N, if larger than M_Z, can presently mainly be probed in radiative corrections (loops). A traditional approach was mostly limited to hypothetical lepton flavor-violating processes such as $\mu\to e\gamma$, $\mu,\tau\to ee^+e^-$, $Z\to e^\pm\mu^\mp$, etc. [3,7–14]. We reviewed constraints from these processes in Sec. IV.

NHL's could also induce (again via radiative corrections) deviations from the SM in currently observed processes, such as those we have previously considered: the leptonic widths of the Z boson Γ_{ll}, lepton universality-breaking parameter $U_{\rm br}$, and the mass of the W boson M_W. The effect of the NHL mass M_N in such radiative corrections is, on the one hand, suppressed by small mixings; on the other hand, it is enhanced due to nondecoupling, the violation of the Appelquist-Carazzone theorem [17]. These competing tendencies are reflected by the typical behavior of the dominant terms,

$$\sim(\tau\tau_{\rm mix})^2M_N^2. \tag{45}$$

To make up for the small mixings, only NHL's with masses in the TeV range can lead to significant deviations from the SM. In the case of one mixing, $\tau\tau_{\rm mix}$, dominating, we found [see Eq. (40)] the following approximate dependence of M_N on $\tau\tau_{\rm mix}$ (2σ level):

$$M_N\leqslant 4.3\times\frac{0.033}{\tau\tau_{\rm mix}}\ \text{TeV}, \tag{46}$$

which arises from the consideration of Z leptonic decays. We also found some sensitivity of the W mass to NHL mass and mixings, but these are quite dependent on the top quark mass so we cannot summarize them in the same way.

These limits on M_N are only matched by those from $\mu\to eee$. The flavor-violating decay rates for τ, which we reviewed in Sec. IV, and for the Z boson, derived in Sec. IV, are below the current experimental sensitivity. Moreover, the $\mu\to eee$ decay depends only on $ee_{\rm mix}$ and $e\mu_{\rm mix}$, two of the six mixing parameters, and may be unobservable if $ee_{\rm mix}$ and/or $e\mu_{\rm mix}$ are very small. The inequality [Eq. (5)] can further suppress the flavor-violating processes against the flavor-conserving ones via the ''conspiracy of the phases'' in the sum of complex terms making up the flavor-violating parameters.

For these reasons, the first signatures of neutral heavy leptons could come from flavor-conserving observables. At this time, LEP has stopped its runs at the Z-peak energy and is running at $130-140$ GeV. It will eventually be producing W pairs which will allow the mass M_W to be measured with a precision of 0.044 GeV [25] (currently $M_W=80.410\pm0.180$ [26]). Combined with more precise measurements of the top quark mass we might be in a position to place even more stringent limits on NHL masses and mixings from our prediction of M_W.

ACKNOWLEDGMENTS

This work was funded in part by the Natural Sciences and Engineering Research Council of Canada. The authors would like to thank R. K. Carnegie for many useful conversations.

APPENDIX A

The total contribution of the box diagrams [Figs. 1(a)–1(g)] is

$$\begin{aligned}\mathcal{M}_{\rm box}&=\mathcal{M}_{Ze_W\mu}+\mathcal{M}_{W\nu_Z\nu}+\mathcal{M}_{W\nu_ZN}+\mathcal{M}_{WNZ\nu}+\mathcal{M}_{WNZN}+\mathcal{M}_{\phi NZN}+\mathcal{M}_{WNHN}+\mathcal{M}_{WN\chi N}+\mathcal{M}_{\phi NHN}+\mathcal{M}_{\phi N\chi N}+\mathcal{M}_{Z\nu W\mu}\\&\quad+\mathcal{M}_{ZNW\mu}+\mathcal{M}_{We_Z\nu}+\mathcal{M}_{We_ZN}\\&=\mathcal{M}_{\rm tree}\frac{\alpha}{4\pi}\left\{\frac{-1}{4s_W^2c_W^2}M_W^2[4(-\tfrac{1}{2}+s_W^2)^2\mathcal{I}_0+\mathcal{I}_0(1-\mu\mu_{\rm mix})(1-ee_{\rm mix})+\mathcal{I}_1(M_Z)(1-\mu\mu_{\rm mix})ee_{\rm mix}\right.\\&\quad+\mathcal{I}_1(M_Z)\mu\mu_{\rm mix}(1-ee_{\rm mix})+\mathcal{I}_2(M_Z)ee_{\rm mix}\mu\mu_{\rm mix}]+\frac{1}{4s_W^2}M_N^4\left[\frac{1}{c_W^2}\mathcal{I}_3(M_Z)+\mathcal{I}_3(M_H)+\mathcal{I}_3(M_Z)\right.\\&\quad\left.\left.-\frac{1}{4M_W^2}\mathcal{I}_2(M_H)-\frac{1}{4M_W^2}\mathcal{I}_2(M_Z)\right]ee_{\rm mix}\mu\mu_{\rm mix}+\frac{2(-1/2+s_W^2)}{s_W^2c_W^2}M_W^2[\mathcal{I}_0(1-ee_{\rm mix})+\mathcal{I}_1(M_Z)ee_{\rm mix}\right.\\&\quad\left.+\mathcal{I}_0(1-\mu\mu_{\rm mix})+\mathcal{I}_1(M_Z)\mu\mu_{\rm mix}]\right\},\end{aligned} \tag{A1}$$

where the integrals $\mathcal{I}_0,\mathcal{I}_1(m),\mathcal{I}_2(m),\mathcal{I}_3(m)$ are

$$\mathcal{I}_0=\frac{(4\pi)^2}{i}\int\frac{d^4k}{(2\pi)^4}\frac{1}{k^2(k^2-M_W^2)(k^2-M_Z^2)}=\frac{1}{M_Z^2-M_W^2}\ln\frac{M_W^2}{M_Z^2}, \tag{A2}$$

$$\mathcal{I}_1(m)=\frac{(4\pi)^2}{i}\int\frac{d^4k}{(2\pi)^4}\frac{1}{(k^2-M_N^2)(k^2-M_W^2)(k^2-m^2)}=\frac{1}{m^2-M_W^2}\left\{\ln\frac{M_W^2}{m^2}+\frac{M_N^2}{M_W^2-M_N^2}\ln\frac{M_W^2}{M_N^2}-\frac{M_N^2}{m^2-M_N^2}\ln\frac{m^2}{M_N^2}\right\}, \tag{A3}$$

$$\begin{aligned}\mathcal{I}_2(m)&=\frac{(4\pi)^2}{i}\int\frac{d^4k}{(2\pi)^4}\frac{k^2}{(k^2-M_N^2)^2(k^2-M_W^2)(k^2-m^2)}\\&=\frac{1}{m^2-M_W^2}\left\{\frac{1}{1-(M_W^2/M_N^2)}+\frac{(M_W^4/M_N^4)\ln(M_W^2/M_N^2)}{(1-(M_W^2/M_N^2))^2}-\frac{1}{1-(m^2/M_N^2)}-\frac{(m^4/M_N^4)\ln(m^2/M_N^2)}{(1-(m^2/M_N^2))^2}\right\},\end{aligned} \tag{A4}$$

$$\begin{aligned}\mathcal{I}_3(m)&=\frac{(4\pi)^2}{i}\int\frac{d^4k}{(2\pi)^4}\frac{1}{(k^2-M_N^2)^2(k^2-M_W^2)(k^2-m^2)}\\&=\frac{1}{m^2-M_W^2}\left\{\frac{1}{M_N^2-M_W^2}+\frac{M_W^2\ln(M_W^2/M_N^2)}{(M_N^2-M_W^2)^2}-\frac{1}{M_N^2-m^2}-\frac{m^2\ln(m^2/M_N^2)}{(M_N^2-m^2)^2}\right\}.\end{aligned} \tag{A5}$$

The computation of the vertex diagrams [Figs. 2(a)–2(f)] yields

$$\begin{aligned}\mathcal{M}^{\mu}_{\text{vertex}}&=\mathcal{M}_{\mu\nu Z}+\mathcal{M}_{\mu NZ}+\mathcal{M}_{ZW\mu}+\mathcal{M}_{\gamma W\mu}+\mathcal{M}_{WZ\nu}+\mathcal{M}_{WZN}+\mathcal{M}_{\phi ZN}+\mathcal{M}_{WHN}+\mathcal{M}_{\phi HN}+\mathcal{M}_{\phi\chi N}\\&=\mathcal{M}_{\text{tree}}\frac{\alpha}{4\pi}\left\{\frac{2s_W^2-1}{4s_W^2c_W^2}\left(\Delta_{M_Z}-\frac{1}{2}\right)(1-\mu\mu_{\text{mix}})+\frac{2s_W^2-1}{4s_W^2c_W^2}\left(\Delta_{M_Z}-\frac{1}{2}-\frac{M_N^2}{M_Z^2-M_N^2}\ln\frac{M_Z^2}{M_N^2}\right)\mu\mu_{\text{mix}}\right.\\&\quad+\frac{\frac{1}{2}-s_W^2}{s_W^2}\left(3\Delta_{M_W}+\frac{5}{2}+\frac{3}{s_W^2}\ln c_W^2\right)+3\left(\Delta_{M_W}+\frac{5}{6}\right)+\frac{3}{2s_W^2}\left(\Delta_{M_W}+\frac{5}{6}+\frac{1}{s_W^2}\ln c_W^2\right)(1-\mu\mu_{\text{mix}})\\&\quad+\frac{3}{2s_W^2}\left[\Delta_{M_W}+\frac{5}{6}+\frac{1}{s_W^2}\ln c_W^2+\frac{M_N^2}{M_Z^2-M_W^2}v(M_Z)\right]\mu\mu_{\text{mix}}+\frac{1}{2c_W^2}\frac{-M_N^2}{M_Z^2-M_W^2}v(M_Z)\mu\mu_{\text{mix}}\\&\quad+\frac{1}{2s_W^2}\frac{-M_N^2}{M_H^2-M_W^2}v(M_H)\mu\mu_{\text{mix}}+\frac{1}{8s_W^2}\frac{M_N^2}{M_W^2}\left[\Delta_{M_W}+\frac{3}{2}-\frac{M_H^2}{M_W^2-M_H^2}\ln\frac{M_W^2}{M_H^2}+\frac{M_N^2}{M_H^2-M_W^2}v(M_H)\right]\mu\mu_{\text{mix}}\\&\quad\left.+\frac{1}{8s_W^2}\frac{M_N^2}{M_W^2}\left[\Delta_{M_W}+\frac{3}{2}-\frac{M_Z^2}{M_W^2-M_Z^2}\ln\frac{M_W^2}{M_Z^2}+\frac{M_N^2}{M_Z^2-M_W^2}v(M_Z)\right]\mu\mu_{\text{mix}}\right\},\end{aligned} \tag{A6}$$

where

$$v(m)=\ln\frac{M_W^2}{m^2}+\frac{M_N^2}{M_W^2-M_N^2}\ln\frac{M_W^2}{M_N^2}-\frac{M_N^2}{m^2-M_N^2}\ln\frac{m^2}{M_N^2}. \tag{A7}$$

The part of the charged lepton self-energy which we specifically use in the text is

$$\Sigma_L^{\phi N} = + \frac{\alpha}{16\pi s_W^2} ll_{\rm mix} \frac{M_N^2}{M_W^2}\left[\Delta_\mu + \frac{3}{2} - 2\ln M_N\right]. \tag{A8}$$

The left-handed part of the neutrino self-energy (Fig. 5) is given by

$$\begin{aligned}
\Sigma_L^{\nu_l} &= \Sigma_L^H(p) + \Sigma_L^\chi(p) + \Sigma_L^{Z,N}(p) + \Sigma_L^{Z,\nu}(p) + \Sigma_L^W(p) \\
&= \frac{\alpha}{2\pi}(1 - ll_{\rm mix})\left\{ \frac{1}{8s_W^2} ll_{\rm mix} \frac{M_N^2}{M_W^2}\left[\frac{1}{2}\Delta_\mu + B_0^{fin}(p;M_H,M_N) + B_1^{fin}(p;M_H,M_N)\right]\right. \\
&\quad + \frac{1}{8s_W^2} ll_{\rm mix} \frac{M_N^2}{M_W^2}\left[\frac{1}{2}\Delta_\mu + B_0^{fin}(p;M_Z,M_N) + B_1^{fin}(p;M_Z,M_N)\right] \\
&\quad + \frac{1}{4s_W^2 c_W^2} ll_{\rm mix}\left[\frac{1}{2}\Delta_\mu - \frac{1}{2} + B_0^{fin}(p;M_Z,M_N) + B_1^{fin}(p;M_Z,M_N)\right] \\
&\quad + \frac{1}{4s_W^2 c_W^2}(1 - ll_{\rm mix})\left[\frac{1}{2}\Delta_\mu - \frac{1}{2} + B_0^{fin}(p;M_Z,0) + B_1^{fin}(p;M_Z,0)\right] \\
&\quad \left. + \frac{1}{2s_W^2}\left[\frac{1}{2}\Delta_\mu - \frac{1}{2} + B_0^{fin}(p;M_W,m_l\to 0) + B_1^{fin}(p;M_W,m_l\to 0)\right]\right\}.
\end{aligned} \tag{A9}$$

Here, $s = p^2 = 0 \ll M_H^2, M_Z^2, M_W^2, M_N^2$

The functions B_0 and B_1 are defined as ($\Delta = 2/\epsilon - \gamma - \ln\pi$):

$$B_0(p;m_1,m_2) = \int \frac{d^n q}{i\pi^2} \frac{1}{(q^2 - m_1^2 + i\epsilon)[(q-p)^2 - m_2^2 + i\epsilon]} = \Delta + B_0^{fin}(p;m_1,m_2),$$

$$B_0^{fin}(p;m_1,m_2) = -\int_0^1 dx\ \ln[p^2x^2 + m_1^2 - (p^2 + m_1^2 - m_2^2)x],$$

$$B_\mu(p;m_1,m_2) = \int \frac{d^n q}{i\pi^2} \frac{q_\mu}{(q^2 - m_1^2 + i\epsilon)[(q-p)^2 - m_2^2 + i\epsilon]} = -p_\mu B_1,$$

$$B_1(p;m_1,m_2) = -\frac{1}{2}\Delta + B_1^{fin}(p;m_1,m_2),$$

$$B_1^{fin}(p;m_1,m_2) = \int_0^1 dx\ \ln[p^2x^2 + m_1^2 - (p^2 + m_1^2 - m_2^2)x]x. \tag{A10}$$

For $s = p^2$ small with respect to m_1^2, m_2^2, m^2, we have

$$B_0(p;m_1,m_2) = 1 - \frac{m_1^2 + m_2^2}{m_1^2 - m_2^2}\ln\frac{m_1}{m_2} - \ln m_1 - \ln m_2 + O(s), \quad B_0(p;0,m) = 1 - 2\ln m + O(s),$$

$$B_1(p;m_1,m_2) = \frac{1}{2}\frac{1}{m_2^2 - m_1^2}\left[\frac{m_1^2 + m_2^2}{2} - \frac{m_1^2 m_2^2}{m_1^2 - m_2^2}\ln\frac{m_1^2}{m_2^2}\right] - \frac{1}{2}B_0(p;m_1,m_2), \quad B_1(p;0,m) = -\frac{1}{4} + \ln m + O(s). \tag{A11}$$

APPENDIX B

Here, we prove Eq. 22, $\Lambda_{\phi HN} + \Lambda_{\phi\chi N} + \delta Z_L^{\phi N} = 0$, using Eq. (21).

We note the vertex $V_{\phi\phi N}^\gamma$ [Fig. 4(c)] is given as

$$\begin{aligned}
V_{\phi\phi N}^\gamma &\equiv ie\gamma_\mu F_V^{\phi\phi N} - ie\gamma_\mu\gamma_5 F_A^{\phi\phi N} \\
&= \sum_a \int \frac{d^n q}{(2\pi)^n} \frac{+ig_2}{\sqrt{2}M_W}(K_H)_{la} M_N \frac{1+\gamma_5}{2} \frac{i}{\not q - \not p_1 - M_N} \frac{+ig_2}{\sqrt{2}M_W}(K_H^\dagger)_{al} M_N \\
&\quad \times \frac{1-\gamma_5}{2} \frac{i}{(q - p_1 - p_2)^2 - M_W^2} \frac{i}{q^2 - M_W^2} ie(-2q + p_1 + p_2)_\mu .
\end{aligned} \tag{B1}$$

If we now return from the γll vertex to the $W\mu\nu$ vertex [Fig. 2(f)], we have

$$V^W_{\phi HN}=\sum_a \int \frac{d^nq}{(2\pi)^n}\frac{-ig_2}{2M_W}M_N(K_L^\dagger K_H)_{ia}\frac{1+\gamma_5}{2}\frac{i}{\not q-\not p_1-M_N}\frac{+ig_2}{\sqrt{2}M_W}(K_H^\dagger)_{al}M_N$$
$$\times\frac{1-\gamma_5}{2}\frac{i}{(q-p_1-p_2)^2-M_H^2}\frac{i}{q^2-M_W^2}\frac{ig_2}{2}(+2q-p_1-p_2)_\mu . \tag{B2}$$

A similar expression holds for $V^W_{\phi\chi N}$. The Lorentz structure of Eqs. (B1) and (B2) is the same. In the large M_N limit, M_H and M_W in the propagators are negligible; therefore, the only possible difference between the two vertices comes from constant factors. If we forget for a moment about the mixing factors, it can be easily checked that

$$V^W_{\phi HN}=\frac{\sqrt{2}g_2}{4e}V^\gamma_{\phi\phi N},$$
$$\mathcal{M}_{\phi HN}+\mathcal{M}_{\phi\chi N}\equiv(\Lambda_{\phi HN}+\Lambda_{\phi\chi N})\mathcal{M}_{\rm tree}=\overline{u_{\nu_\mu}}(V^W_{\phi HN}+V^W_{\phi\chi N})u_\mu\frac{ig^{\mu\nu}}{M_W^2}\overline{v_e}\frac{ig_2}{2\sqrt{2}}(K_L)_{ej}\gamma_\nu(1-\gamma_5)v_{\nu_e}$$
$$\Lambda_{\phi HN}+\Lambda_{\phi\chi N}=2F_V^{\phi\phi N}=2F_A^{\phi\phi N}. \tag{B3}$$

Hence [using Eqs. (B3) and (21)],

$$\Lambda_{\phi HN}+\Lambda_{\phi\chi N}+\delta Z_L^{\phi N}=2F_V^{\phi\phi N}+\delta Z_V^{\phi N}+\delta Z_A^{\phi N}=2(F_V^{\phi\phi N}+\delta Z_V^{\phi N})=0. \tag{B4}$$

That is, the two dominant nonstandard contributions from Eq. (16) cancel. To show that the inclusion of the mixing factors will not affect Eq. (B4), note that the mixing factor for the $W\mu\nu$ vertex, which we denote as k_1, is related to that of the γll vertex, denoted as k_2, in the approximation in which flavor-violating mixing factors $e\mu_{\rm mix},\tau\mu_{\rm mix}$, $e\tau_{\rm mix}$ are vanishing, as follows.

$$k_1=\sum_a (K_H^\dagger)_{a\mu}(K_L^\dagger K_H)_{ia}=(K_L^\dagger)_{ie}\sum_a (K_H)_{ea}(K_H^\dagger)_{a\mu}+(K_L^\dagger)_{i\mu}\sum_a (K_H)_{\mu a}(K_H^\dagger)_{a\mu}+(K_L^\dagger)_{i\tau}\sum_a (K_H)_{\tau a}(K_H^\dagger)_{a\mu}$$
$$=(K_L^\dagger)_{ie}e\mu_{\rm mix}+(K_L^\dagger)_{i\mu}\mu\mu_{\rm mix}+(K_L^\dagger)_{i\tau}\tau\mu_{\rm mix}=(K_L^\dagger)_{i\mu}\mu\mu_{\rm mix}=(K_L^\dagger)_{i\mu}k_2. \tag{B5}$$

The remaining factor $(K_L^\dagger)_{i\mu}$ is absorbed into $\mathcal{M}_{\rm tree}$ as required.

[1] G. Bhattacharya, P. Kalyniak, and I. Melo, Phys. Rev. D **51**, 3569 (1995).
[2] R. N. Mohapatra and J. W. F. Valle, Phys. Rev. D **34**, 1642 (1986).
[3] J. Bernabéu, A. Santamaria, J. Vidal, A. Mendez, and J. W. F. Valle, Phys. Lett. B **187**, 303 (1987).
[4] D. Wyler and L. Wolfenstein, Nucl. Phys. **B218**, 205 (1983).
[5] B. A. Kniehl and A. Pilaftsis, Nucl. Phys. **B474**, 286 (1996).
[6] Particle Data Group, L. Montanet *et al.*, Phys. Rev. D **50**, 1173 (1994).
[7] L. N. Chang, D. Ng, and J. N. Ng, Phys. Rev. D **50**, 4589 (1994).
[8] D. Ng and J. N. Ng, Phys. Lett. B **331**, 371 (1994).
[9] M. C. Gonzalez-Garcia and J. W. F. Valle, Mod. Phys. Lett. A **7**, 477 (1991).
[10] A. Ilakovac and A. Pilaftsis, Nucl. Phys. **B437**, 491 (1995).
[11] D. Tommasini, G. Barenboim, J. Bernabeu, and C. Jarlskog, Nucl. Phys. **B444**, 451 (1995).
[12] N. Rius and J. W. F. Valle, Phys. Lett. B **246**, 249 (1990).
[13] J. G. Korner, A. Pilaftsis, and K. Schilcher, Phys. Lett. B **300**, 381 (1993).
[14] A. Pilaftsis, Mod. Phys. Lett. A **9**, 3595 (1994).
[15] E. Nardi, E. Roulet, and D. Tommasini, Phys. Lett. B **327**, 319 (1994).
[16] F. Matorras, in *Proceedings of XXXI Rencontres de Moriond, Electroweak Interactions and Unified Theories*, Les Ares, France, 1996 (Editions Frontières, Gif-sur-Yvette, 1996).
[17] T. Appelquist and J. Carazzone, Phys. Rev. D **11**, 2856 (1975).
[18] W. Hollik, Fortschr. Phys. **38**, 165 (1990).
[19] J. C. Ward, Phys. Rev. **78**, 1824 (1950); J. C. Taylor, Nucl. Phys. **B33**, 436 (1971); A. A. Slavnov, Theor. Math. Phys. **10**, 99 (1972).
[20] A. Denner and T. Sack, Nucl. Phys. **B347**, 203 (1990).
[21] A. Olchevski, in *Proceedings of the International Europhysics Conference on High Energy Physics*, Brussels, 1995 (World Scientific, Singapore, 1995).
[22] J. Bernabéu, J. G. Körner, A. Pilaftsis, and K. Schilcher, Phys. Rev. Lett. **71**, 2695 (1993).
[23] A. Pilaftsis, Z. Phys. C **55**, 275 (1992).
[24] John Jowett, in *Proceedings of the Tau-Charm Factory Workshop*, Stanford, California, 1989, edited by Lydia V. Beers (SLAC Report No. 343, Stanford, 1989), p. 7; Y. S. Tsai, Phys. Rev. D **51**, 3172 (1995).
[25] R. K. Carnegie (private communication); G. Altarelli, T. Sjostrand, and F. Zwirner, report of the Workshop on Physics at LEP2 (unpublished), Report No. hep-ph/9602352 (unpublished).
[26] CDF Collaboration, F. Abe *et al.*, Phys. Rev. Lett. **75**, 11 (1995).